Struct Bond
DOI: 10.1007/430_2015_5001

4f-Clusters for Cryogenic Magnetic Cooling

Yan-Cong Chen, Jun-Liang Liu, and Ming-Liang Tong

Abstract Based on the magnetocaloric effect (MCE), cryogenic magnetic cooling is one of the most promising applications of molecule-based magnets. In recent years, 4f-clusters played important roles and set up several records in such area, some of which exhibit large and promising cryogenic MCE catching up the commercial coolant GGG. Here in this chapter, we focus on the structure–magnetocaloric correlations of 4f-clusters and 4f-cluster-based coordination polymers for use as cryogenic magnetic coolants. The assembly strategies are introduced and discussed on the purpose of obtaining high performance 4f-clusters for cryogenic magnetic cooling. Then, the recent development is summarized and accompanied by the discussion on representative examples. Finally, the outlooks about the future research directions in this area are made.

Keywords Cluster compounds • Lanthanide • Magnetic coolant • Magnetocaloric effect • Magnetocaloric material

Contents

Y.-C. Chen, J.-L. Liu, and M.-L. Tong (✉)
Key Laboratory of Bioinorganic and Synthetic Chemistry of Ministry of Education, School of Chemistry and Chemical Engineering, Sun Yat-sen University, Guangzhou 510275, Peoples Republic of China
e-mail: tongml@mail.sysu.edu.cn

Abbreviations

3-TCA	Thiophene-3-carboxylic acid
CAA	Chloroacetic acid
DMC	*N*,*N*′-dimethylcarbamic acid anions
H_2DPA	Diphenic acid
H_3dhpimp	(*E*)-2-(2,3-dihydroxypropylimino)methyl)-phenol
H_4bmhcp	2,6-Bis[(3-methoxysalicylidene)hydrazinecarbonyl]pyridine
HNA	Nicotinic acid
mvandeta	*N*,*N*′,*N*″-Trimethyl-*N*,*N*″-bis(2-hydroxy-3-methoxy-5-methylbenzyl)-diethylenetriamine
thmeH_3	Tris(hydroxymethyl)ethane
tpaH	Triphenylacetic acid

1 Introduction

The history of cryogenic MCE began in the early 1930s using paramagnetic salts to obtain ultra-low temperature down to the sub-Kelvin level by adiabatic demagnetization [1, 2]. Many different kinds of materials have been studied in the following years, including metals, alloys and intermetallic compounds, and the gadolinium gallium garnet ($Gd_3Ga_5O_{12}$, GGG) is chosen nowadays as the commercial cryogenic magnetic coolant.

As a major field in molecular magnetism, cryogenic magnetic cooling using molecule-based materials grew rapidly in the last decade [3–10]. The adventure began with the 3d metal clusters with high spin (*S*); however, their performance was limited by strong magnetic coupling and/or large magnetic anisotropy. Later, 4f ions, especially the Gd(III) ions, were intensively studied in both 3d-4f systems and pure 4f systems, leading to significant breakthroughs on not only the molecular clusters but also the cluster-based coordination polymers with large cryogenic MCE, catching up the commercial coolant GGG.

Here in this chapter, we focus on the 4f-clusters for cryogenic magnetic cooling. Firstly, the basic theory and assembly strategies are introduced, followed by the case study on the structure–magnetocaloric correlations on recent development of discrete 4f-clusters and the 4f-cluster-based coordination polymers. Finally, the prospect and challenges are concluded.

2 Basic Theory

The MCE of a magnetic coolant can be evaluated by two key parameters, namely – ΔS_M (isothermal magnetic entropy change) and ΔT_{ad} (adiabatic temperature change). For a magnetic insulator with negligible electronic entropy, the total

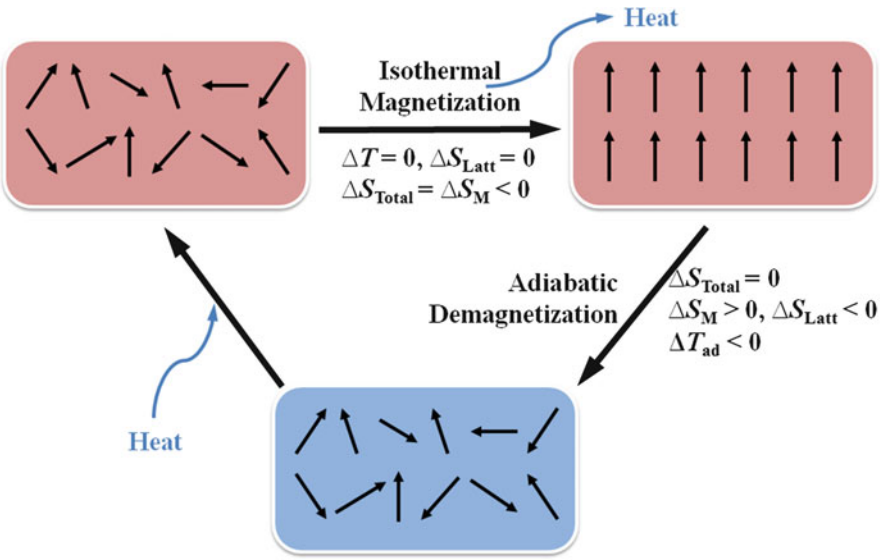

Scheme 1 The isothermal magnetization process and adiabatic demagnetization process in magnetic cooling

entropy (S_{Total}) only comprises the field-dependent magnetic entropy (S_M) and the field-independent lattice entropy (S_{Latt}) [11, 12].

$$S_{Total}(T,H) = S_M(T,H) + S_{Latt}(T) \quad (1)$$

During an isothermal magnetization process, the temperature and the lattice entropy are unchanged ($\Delta T = 0$, $\Delta S_{Latt} = 0$) whereas the increasing magnetic field removes the degeneracies of the energy levels and leads to a decrease in the magnetic entropy ($\Delta S_{Total} = \Delta S_M < 0$), and the heat produced in this process should be released to environment.

Then, during an adiabatic demagnetization process, the total entropy is unchanged ($\Delta S_{Total} = 0$), whereas the degeneracies of the energy levels are restored and lead to an increase in the magnetic entropy ($\Delta S_M > 0$). As compensation, the lattice entropy must decrease ($\Delta S_{Latt} < 0$) and appear as a temperature drop ($\Delta T_{ad} < 0$). By running such a system in reversible magnetothermal cycles, heat can be pumped out continuously and achieve the magnetic cooling (Scheme 1).

To evaluate a given material for magnetic cooling, the $-\Delta S_M$ and ΔT_{ad} parameters can be calculated from isothermal magnetization using the Maxwell equation, $[\partial S_M(T,H)/\partial H]_T = [\partial M(T,H)/\partial T]_H$, and from heat capacity applying the integration either from absolute zero or from the high-temperature end [10]. In addition, the ΔT_{ad} can also be directly measured by running a pseudo-adiabatic magnetization/demagnetization process.

3 Assembly Strategies

To obtain high performance 4f-clusters for cryogenic magnetic cooling, the most primary requirement is the high spin, because the full magnetic entropy is defined as $S_M = R\ln(2S+1)$ for a magnetic system with a well-isolated spin-only S, and this will act as the upper limit of the maximum ΔS_M. Since the zero-field splitting, spin–orbit coupling and magnetic interactions can largely reduce the degeneracies, Gd(III) is the most promising candidate owing to the large $S = {}^7/_2$ single-ion spin from the $4f^7$ electron configuration and the negligible anisotropy without orbital contribution. In addition, the magnetic interactions between Gd(III) ions are usually weak and thus extremely suitable for a large MCE. If the complex is properly designed, a maximum $-\Delta S_m$ value of $R\ln(8)$ or $2.08R$ can be obtained for each Gd(III).

However, things are not so simple as the Gd(III) ion cannot form a compound all on its own – ligands and/or counter ions are necessary to balance the charge and provide the coordination environment. Although these nonmagnetic components do not have direct influence on magnetic cooling, they inevitably take up weight and space, thus lowering the performances when evaluating the MCE in the practical units, such as the gravimetric (J kg^{-1} K^{-1}) and volumetric (mJ cm^{-3} K^{-1}) ones.

The most straightforward and also successful strategy is to select small and light bridging ligands, which increase the metal-to-ligand ratio in the compound. These include the carboxyl groups (-COO^-) and most inorganic anions such as OH^-, CO_3^{2-} and SO_4^{2-}. However, such a strategy is a double-edged sword as the magnetic interactions will become stronger with small bridging ligands, which hinder the full exploitation of magnetic entropy. For the polymeric materials, the long-range magnetic ordering temperature may also be increased.

Combining organic and inorganic ligands in 4f-clusters and 4f-cluster-based coordination polymers is another successful approach to strike a balance between dense structures and strong magnetic interactions. The inorganic core inside the cluster can maximize the density of spin carriers; while the organic ligands on the shell (or as linkers) separate neighbouring clusters and keep the ordering temperature below the working region.

Finally, if the magnetic interactions are inevitable, choosing suitable bridging ligands such as F^- ions to achieve ferromagnetic interactions is much better than antiferromagnetic ones. Indeed, although weak ferromagnetic interactions lower the maximum approachable value of $-\Delta S_m$ compared with paramagnetic cases, the performance at a high temperature and in lower fields can be improved. This is of great significance to practical application as the working field can be provided by the convenient permanent magnets instead of superconducting electromagnets.

4 Recent Development

4.1 4f-Clusters for Cryogenic Magnetic Cooling

The disc-like $\{Gd_7\}$ (Fig. 1), $[Gd_7(OH)_6(thmeH_2)_5(thmeH)(tpa)_6(MeCN)_2](NO_3)_2$ (**1**) [13], was solvothermally synthesized from $Ln(NO_3)_3 \cdot 5H_2O$, the tripodal alcohol tris(hydroxymethyl)ethane ($thmeH_3$) and triphenylacetic acid (tpaH). The central Gd(III) was surrounded by a Gd_6 hexagon with six μ_3-OH groups alternating above and below the plane, and the outer shell is constructed by $thmeH_2^-$, $themH^{2-}$ and tpa^-.

The magnetic interactions between Gd(III) are antiferromagnetic, but the frustrated topology leads to low-lying excited states, thereby yielding a comparable $-\Delta S_M = 23$ J kg^{-1} K^{-1} at 3 K with $\Delta H = 70$ kOe. Although the $-\Delta S_M$ value was quite large at that time, however, it is only equivalent to 10.6*R* compared with the full entropy of 14.6*R* for seven uncoupled Gd(III), thereby demonstrating the need to reduce antiferromagnetic coupling.

Subsequently, the simple and well-known ferromagnetic $\{Gd_2\}$ dimer (Fig. 2) of gadolinium acetate tetrahydrate, $[\{Gd(OAc)_3(H_2O)_2\}_2] \cdot 4H_2O$ (**2**) [14], was evaluated by magnetization, heat capacity and direct measurements to assess its MCE.

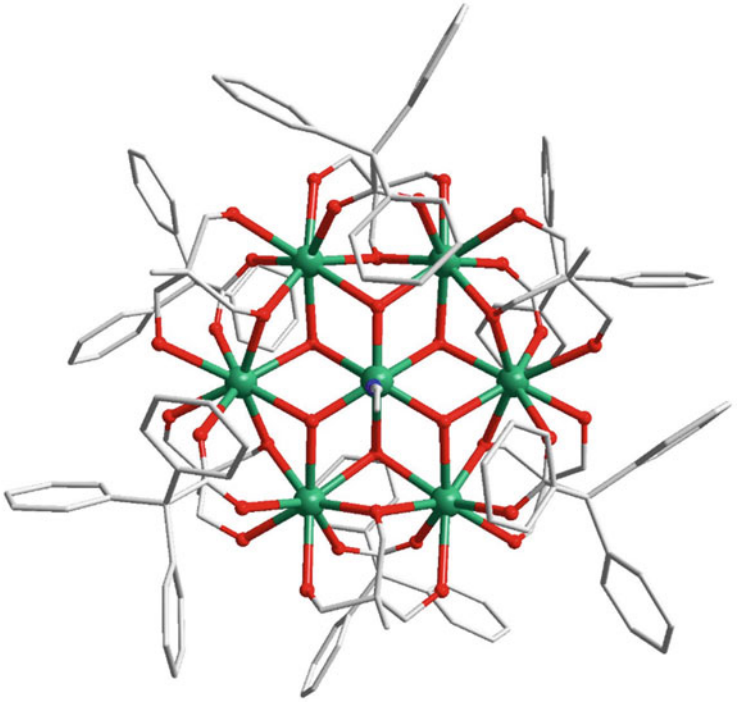

Fig. 1 Crystal structure of $[Gd_7(OH)_6(thmeH_2)_5(thmeH)(tpa)_6(MeCN)_2](NO_3)_2$ (**1**)

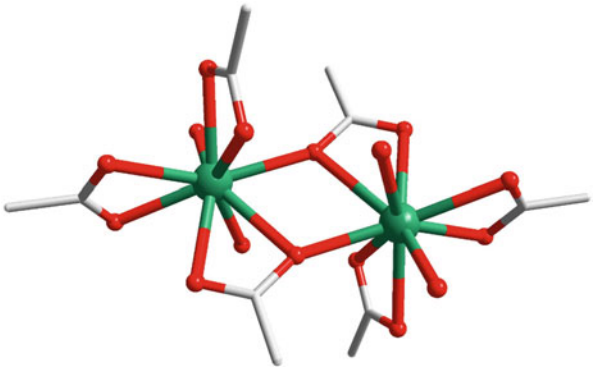

Fig. 2 Crystal structure of $[\{Gd(OAc)_3(H_2O)_2\}_2]\cdot 4H_2O$ (**2**)

The ferromagnetic interactions in this compound lead to nice performance with a relatively modest $\Delta H = 10$ kOe, namely $-\Delta S_M = 27$ J kg^{-1} K^{-1} at 0.5 K and $\Delta T_{ad} = 3.5$ K. For larger ΔH, the maximum value of $-\Delta S_M$ exceeds 40 J kg^{-1} K^{-1} at 1.8 K with $\Delta H = 70$ kOe, approaching the upper limit of 42.5 J kg^{-1} K^{-1} corresponding to $4.16R$. Finally, the magnetic ordering T_c was estimated by a Metropolis Monte Carlo simulation as 0.18 K, far below the working region. Although this complex is somewhat similar to the gadolinium sulphate octahydrate, $Gd_2(SO_4)_3\cdot 8H_2O$, used at the very first age of cryogenic magnetic cooling, it is believed that this $\{Gd_2\}$ dimer possesses quite an advantage owing to the intramolecular ferromagnetic coupling ($J = 0.068(2)$ K). Recently, a Zn–Gd cluster complex, $[Zn_2Gd_2(mvandeta)_2(CO_3)_2(NO_3)_2]\cdot 4CH_3OH$ (**3**) [15], was reported with similar Gd–Gd bridging fragments. A weak intra-dimer ferromagnetic interaction of $J = 0.038(2)$ K was found. Similarly, the maximal value of $-\Delta S_M = 18.5$ J kg^{-1} K^{-1} at 1.9 K with $\Delta H = 70$ kOe was close to the full entropy content; however, the diamagnetic Zn^{2+} and bulky ligands lead to the large difference in the performance between $\{Zn_2Gd_2\}$ and $\{Gd_2\}$.

The following dimer $[Gd_2(OAc)_2(Ph_2acac)_4(MeOH)_2]$ (**4**) and tetranuclear $[Gd_4(OAc)_4(acac)_8(H_2O)_4]$ (**5**) clearly demonstrated how the metal-to-ligand ratio can affect the MCE properties (Fig. 3) [16]. Both complexes are ferromagnetically coupled, namely $J = 0.04$ cm^{-1} for **4** and $J_1 = J_2 = 0.02$ cm^{-1} for **5**. The maximum values of $-\Delta S_M$ reach$1.98R$ and $1.96R$, respectively, very close to the full entropy of $2.08R$. However, the difference arises from the Mw/N_{Gd}, namely 695 g mol^{-1} for **4** and 432.5 g mol^{-1} for **5**. Therefore, the $-\Delta S_M$ values are largely differed as 23.7 J kg^{-1} K^{-1} at 2.4 K with $\Delta H = 70$ kOe for **4** and 37.7 J kg^{-1} K^{-1} at 2.4 K with $\Delta H = 70$ kOe for **5**, respectively.

The square-based pyramid $[Gd_5O(O^iPr)_{13}]$ (**6**, Fig. 4) was obtained from reactions between anhydrous $LnCl_3$ and isopropanol (^{i}PrOH) and belongs to the $\{Ln_5\}$ family [17]. The μ_5-O and μ_3-O^{i}Pr provide efficient routes for intramolecular antiferromagnetic coupling with a frustrated $J = -0.085$ cm^{-1}. Although the maximum $-\Delta S_M$ of 34 J kg^{-1} K^{-1} can be achieved at 3 K with $\Delta H = 70$ kOe, it is well

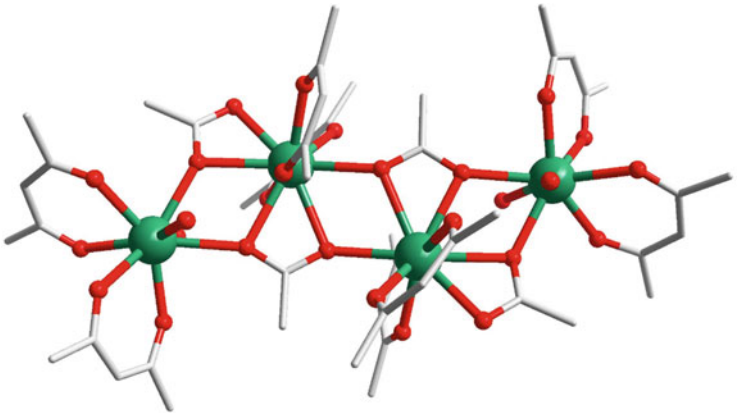

Fig. 3 Crystal structure $[Gd_4(OAc)_4(acac)_8(H_2O)_4]$ (**5**)

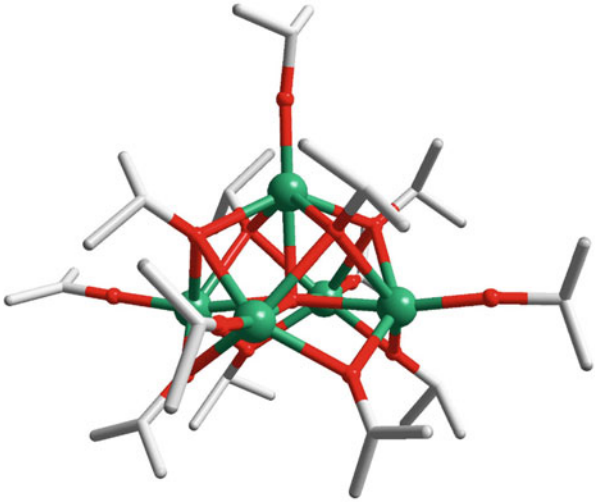

Fig. 4 Crystal structure of $[Gd_5O(O^iPr)_{13}]$ (**6**)

below the limit value of 55 J kg^{-1} K^{-1}. Apart from the relatively strong magnetic coupling, the high magnetic anisotropy that leads to nice SMM behaviour for Dy and Ho derivatives actually plays a negative role for Gd as a magnetic coolant.

By the reaction of $Ln(NO_3)_3 \cdot 6H_2O$, HO_2C^tBu, $H_2O_3P^tBu$ and a mild base $^iPrNH_2$ in ^iBuOH, the "horseshoe" 4f-phosphonate clusters, $(NH_3{}^iPr)_2$ $[Gd_8(O_3P^tBu)_6(\mu_3\text{-}OH)_2(H_2O)_2(HO^iBu)(O_2C^tBu)_{12}]$ (**7**) [18], can be isolated. The structure of this complex comprises a $\{Gd_8P_6\}$ core (Fig. 5), while the outer shell is encapsulated by hydrophobic *tert*-butyl groups. The clusters are well isolated with weak but antiferromagnetic interactions among Gd(III) ions, which were evaluated based on

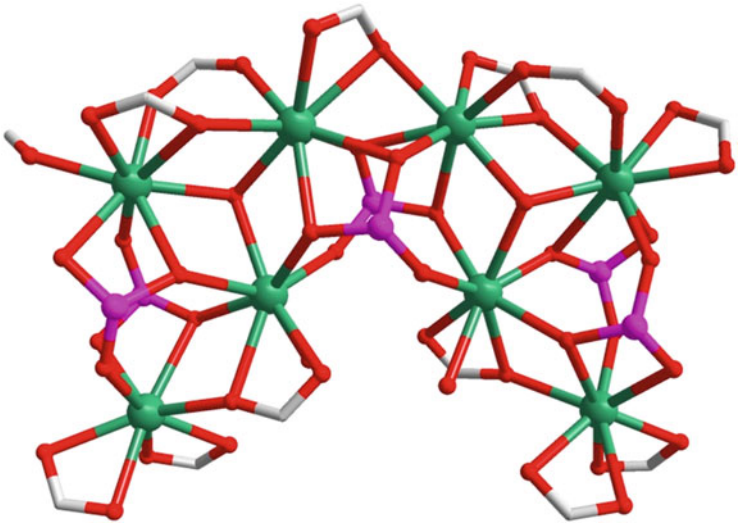

Fig. 5 Crystal structure of $[Gd_8(O_3P^tBu)_6(\mu_3\text{-}OH)_2(H_2O)_2(HO^iBu)(O_2C^tBu)_{12}](NH_3{}^iPr)_2$ (**7**)

an equivalent neighbouring exchange parameter of $J = -0.03\ cm^{-1}$. The maximum value of $-\Delta S_M$ is 32.3 J kg^{-1} K^{-1} at 3 K with $\Delta H = 70$ kOe, which is lower than the expected value of 45.9 J kg^{-1} K^{-1} for eight uncoupled Gd(III). Although the $-\Delta S_M$ value itself is moderate, this case was the first magnetic entropy study on the 4f-phosphonate clusters and opened a new category thereafter.

An unprecedented {Gd_{10}} cluster comprising the $[Gd_{10}(\mu_3\text{-}OH)_8]^{22+}$ core, $[Gd_{10}(3\text{-}TCA)_{22}(\mu_3\text{-}OH)_8(H_2O)_4]$ (**8**, Fig. 6) [19], is formed via a hydrothermal reaction between Gd_2O_3 and 3-TCA. The Gd_2O_3 acts as both a slow-release Gd(III) source and a pH regulator of the system, leading to an inorganic core surrounded by the organic shell of 3-TCA. The weak antiferromagnetic interaction with $\theta = -1.78$ K yields $\Delta T_{ad} = 8.7$ K at 2 K and $-\Delta S_M = 31.2$ J kg^{-1} K^{-1} at 3 K with $\Delta H = 70$ kOe, which is close to the calculated value of 37.8 J kg^{-1} K^{-1}, despite the relatively high inorganic component of such compound.

Another decanuclear 4f-cluster, $[Gd_{10}(bmhcp)_5(\mu\text{-}OH)_6(H_2O)_{22}](Cl)_4 \cdot 7H_2O$ (**9**, Fig. 7), can be synthesized using a hydrazine-based ligand H_4bmhcp [20]. The cage can be regarded as a $2 \times [1 \times 5]$ rectangular array, with five ligands categorized into three "rungs" and two "rails". The rung locks were acted by six Gd(III) ions, while each discrete molecule encapsulates three Cl^- ions at the centre by hydrogen bonds. The magnetic interactions between Gd(III) are antiferromagnetic, and the maximum $-\Delta S_M$ is moderate as 37.4 J kg^{-1} K^{-1} at 3 K with $\Delta H = 70$ kOe.

The truncated tetrahedral cluster {Gd_{12}} (Fig. 8), $[Gd_{12}Mo_4O_{16}(Hdhpimp)_6(\mu_3\text{-}OH)_4\ (MeCO_2)_{12}] \cdot 12MeOH \cdot 8H_2O$ (**10**), was solvothermally synthesized with the presence of $(n\text{-}Bu_4N)_4Mo_8O_{26}$ [21]. Four oxometalate ions, $MoO_4{}^{2-}$,

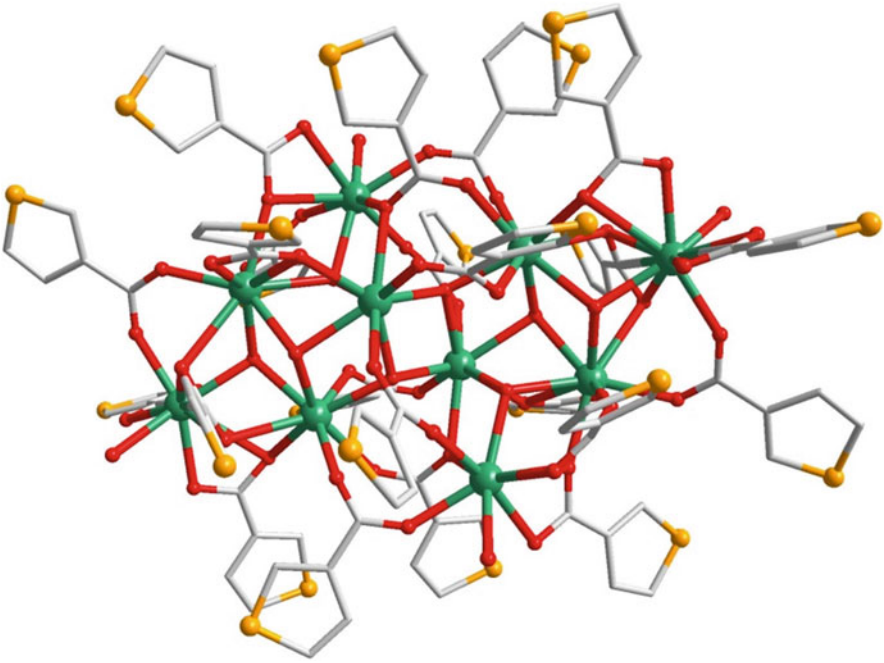

Fig. 6 Crystal structure of $[Gd_{10}(3\text{-}TCA)_{22}(\mu_3\text{-}OH)_8(H_2O)_4]_2$ (**8**)

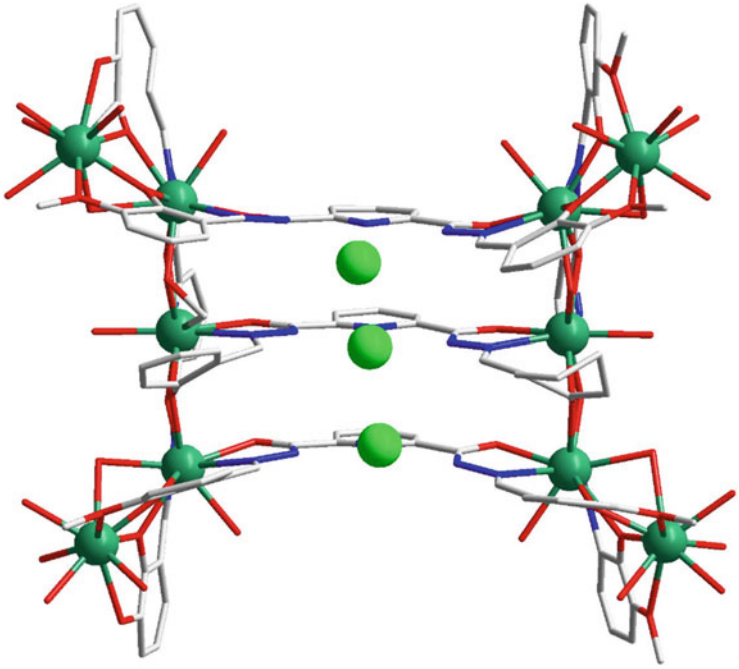

Fig. 7 Crystal structure of $[Gd_{10}(bmhcp)_5(\mu\text{-}OH)_6(H_2O)_{22}]Cl_4 \cdot 7H_2O$ (**9**)

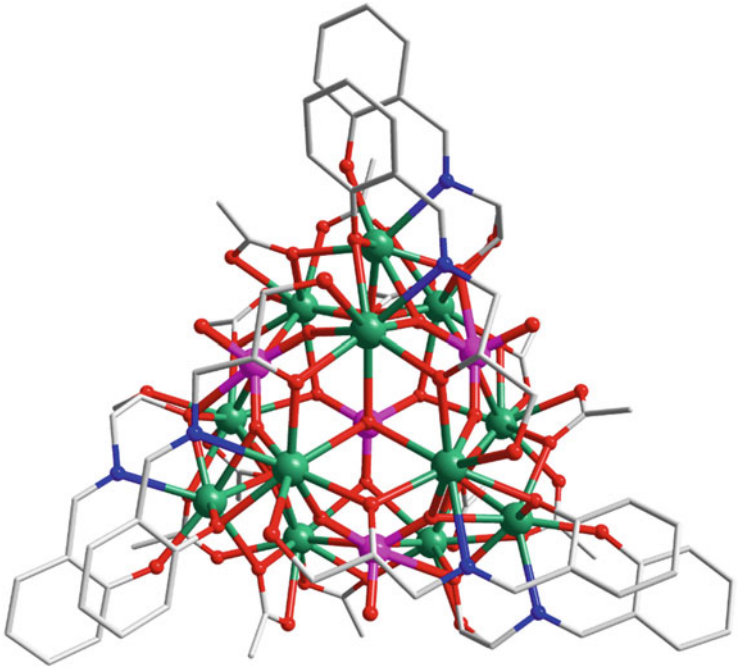

Fig. 8 Crystal structure of $[Gd_{12}Mo_4O_{16}(Hdhpimp)_6(\mu_3\text{-}OH)_4(MeCO_2)_{12}] \cdot 12MeOH \cdot 8H_2O$ (**10**)

were found in the final cluster and served as the templates for the assembly. The magnetic interactions are antiferromagnetic with the exchange constant J estimated as -0.04 K using a Monte Carlo simulation and the finite temperature Lanczos method. The highest $-\Delta S_M$ value reached 35.3 J kg^{-1} K^{-1} at 3 K with $\Delta H = 70$ kOe, close to the calculated value of 41.6 J kg^{-1} K^{-1}.

The capsule-like $\{Gd_{24}\}$, $[Gd_{24}(DMC)_{36}(\mu_4\text{-}CO_3)_{18}(\mu_3\text{-}H_2O)_2] \cdot 6H_2O$ (**11**) [22], comprises DMC and CO_3^{2-} anions which are both in situ generated from DMF and act as coats and bridges, respectively (Fig. 9). It is a rare case of high-nuclearity lanthanide clusters without bridging OH^- groups, thus the antiferromagnetic interactions between Gd(III) ions are quite weak with a small Weiss constant $\theta = -0.16$ K. This combined with the low molecular weight normalized per Gd(III) as 340.39 g mol^{-1} leads to a maximum $-\Delta S_M$ value of 46.1 J kg^{-1} K^{-1} at 2.5 K with $\Delta H = 70$ kOe, approaching the theoretical limit of 52.1 J kg^{-1} K^{-1}. For an anisotropic Dy(III) analogue, however, the maximum $-\Delta S_M$ value declines to only 13.8 J kg^{-1} K^{-1} at 7 K with $\Delta H = 70$ kOe mainly owing to the magnetic anisotropy of Dy(III) ions.

The nanoscale $\{Gd_{38}\}$ cage and $\{Gd_{48}\}$ barrel, i.e., $[Gd_{38}(\mu\text{-}O)(\mu_8\text{-}ClO_4)_6(\mu_3\text{-}OH)_{42}(CAA)_{37}(H_2O)_{36}(EtOH)_6](ClO_4)_{10}(OH)_{17} \cdot 14DMSO \cdot 13H_2O$ (**12**) and $[Gd_{48}(\mu_4\text{-}O)_6(\mu_3\text{-}OH)_{84}(CAA)_{36}(NO_3)_6(H_2O)_{24}(EtOH)_{12}(NO_3)Cl_2]$ $Cl_3 \cdot 6DMF \cdot 5EtOH \cdot 20H_2O$ (**13**) [23], demonstrated the anion-templated synthesis of high-nuclearity lanthanide clusters with large MCEs (Fig. 10). The basic units are

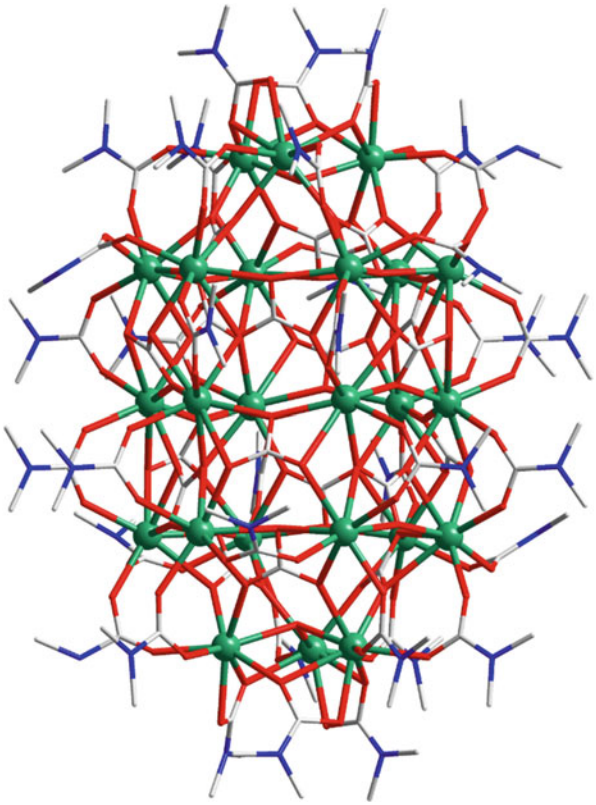

Fig. 9 Crystal structure of $[Gd_{24}(DMC)_{36}(\mu_4\text{-}CO_3)_{18}(\mu_3\text{-}H_2O)_2] \cdot 6H_2O$ (**11**)

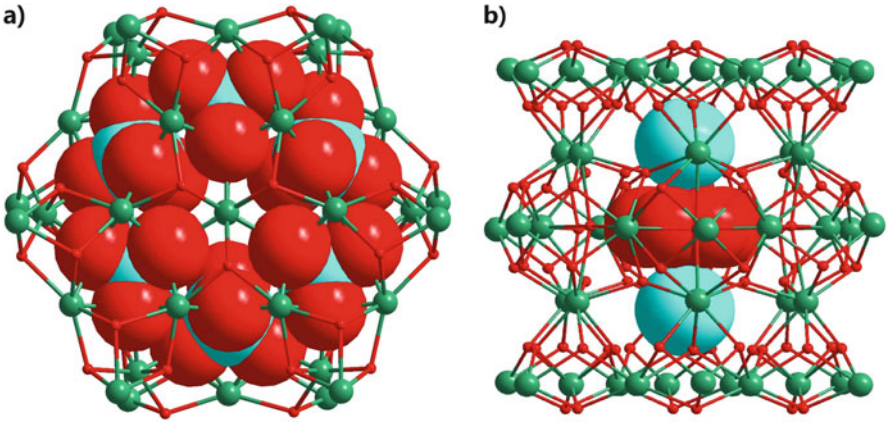

Fig. 10 Crystal structures of **12** (a) and **13** (b)

tetrahedral $\{Gd_4\}$ and/or pyramidal $\{Gd_5\}$, which connected with the anion template and hydroxyl groups into $\{Gd_{38}(ClO_4)_6\}$ for **12** and $\{Gd_{48}Cl_2(NO_3)\}$ for **13**. Both complexes exhibit antiferromagnetic interactions among Gd(III) ions: for **12**, the Weiss constant is $\theta = -2.99$ K and the maximum $-\Delta S_M$ value is 37.9 J kg^{-1} K^{-1} at 1.8 K with $\Delta H = 70$ kOe, while for **13**, $\theta = -3.57$ K and $-\Delta S_M$ increases to 43.6 J kg^{-1} K^{-1} at 1.8 K with $\Delta H = 70$ kOe. Although these are still less than the upper limit of 42 and 50.4 J kg^{-1} K^{-1}, respectively, their relatively high mass densities of 2.689 and 2.769 g cm^{-3} serve as a compensation. When evaluating the values in the volumetric unit, they exhibit much more competitive $-\Delta S_M$ of 102 and 120.7 mJ cm^{-3} K^{-1}, respectively.

The giant 104-Gd complex, $[Gd_{104}(ClO_4)_6(CH_3COO)_{56}(\mu_3\text{-}OH)_{168}(\mu_4\text{-}O)_{30}(H_2O)_{112}](ClO_4)_{22} \cdot 2CH_3CH_2OH \cdot 140H_2O$ (**14**), is the largest known lanthanide-exclusive cluster [24]. This high-nuclearity cluster is synthesized from the hydrolysis of $Gd(ClO_4)_3$ with the presence of acetate, forming a four-shell $Gd_8@Gd_{48}@Gd_{24}@Gd_{24}$ arrangement (Fig. 11). The magnetic interactions are

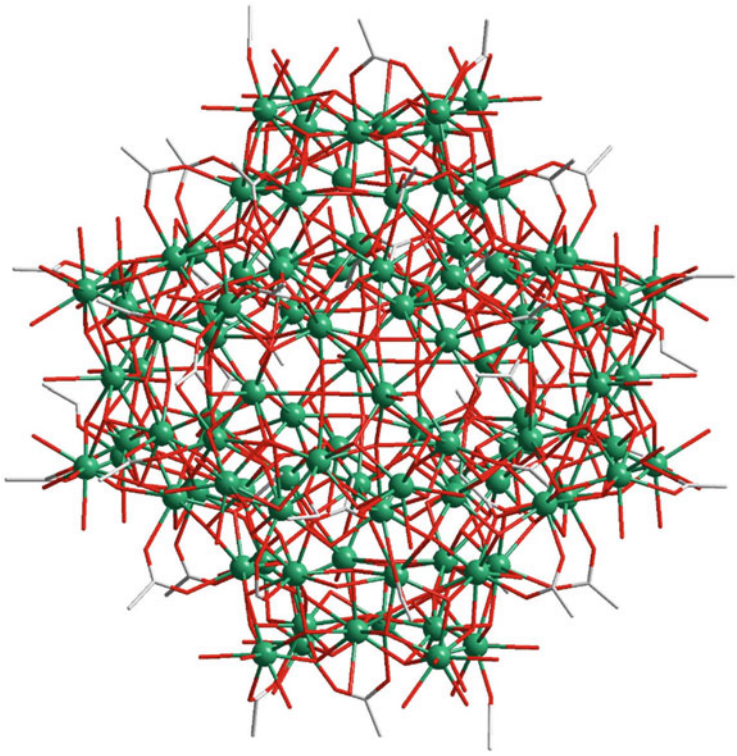

Fig. 11 Crystal structures of $[Gd_{104}(ClO_4)_6(CH_3COO)_{56}(\mu_3\text{-}OH)_{168}(\mu_4\text{-}O)_{30}(H_2O)_{112}](ClO_4)_{22} \cdot 2CH_3CH_2OH \cdot 140H_2O$ (**14**)

also antiferromagnetic with the Weiss constant of $\theta = -4.11$ K, and the maximum $-\Delta S_M$ value is 46.9 J kg^{-1} K^{-1} at 2 K with $\Delta H = 70$ kOe, lower than the anticipated 59.1 J kg^{-1} K^{-1}. However, the large density of 2.945 g cm^{-3} leads to nice $-\Delta S_M$ of 137.2 mJ cm^{-3} K^{-1}, the largest one among 4f-clusters.

4.2 4f-Cluster-Based Coordination Polymers for Cryogenic Magnetic Cooling

The sulphate-based network with distorted cubic $\{Gd_4(\mu_3\text{-}OH)_4\}$ building units, $[Gd_4(SO_4)_4(\mu_3\text{-}OH)_4(H_2O)_4]_n$ (**15**), was synthesized comprising the tetranuclear clusters as 12-connected nodes and the SO_4^{2-} as 4-connected nodes, which lead to a unique (3,12)-connected topological network (Fig. 12) [25]. The magnetic interactions are weakly antiferromagnetic with a negative Weiss constant θ of -1.57 K, and the maximum $-\Delta S_M$ reaches quite a significant value of 51.3 J kg^{-1} K^{-1} (198.9 mJ cm^{-3} K^{-1}) at 2 K with $\Delta H = 70$ kOe owing to the low Mw/N_{Gd} of 288.3 g mol^{-1} and the large density of 3.877 g cm^{-3}.

A similar (3,11)-connected network based on the $\{Gd_4(\mu_3\text{-}OH)_4\}$ building units, $[Gd_4(\mu_4\text{-}SO_4)_3(\mu_3\text{-}OH)_4(\mu\text{-}C_2O_4)(\mu\text{-}H_2O)(H_2O)_4]_n \cdot nH_2O$ (**16**), was synthesized with the in situ generated sulphate and oxalate [26]. This inorganic–organic hybrid framework also exhibits antiferromagnetic interaction with $\theta = -1.57$ K, and the maximum $-\Delta S_M$ value is 51.5 J kg^{-1} K^{-1} (190.5 mJ cm^{-3} K^{-1}) at 2 K with $\Delta H = 70$ kOe, also among the highest ones.

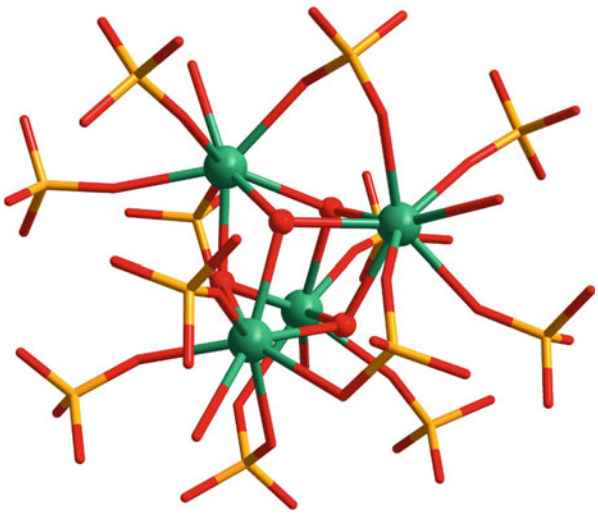

Fig. 12 Crystal structure of $[Gd_4(SO_4)_4(\mu_3\text{-}OH)_4(H_2O)_4]_n$ (**15**)

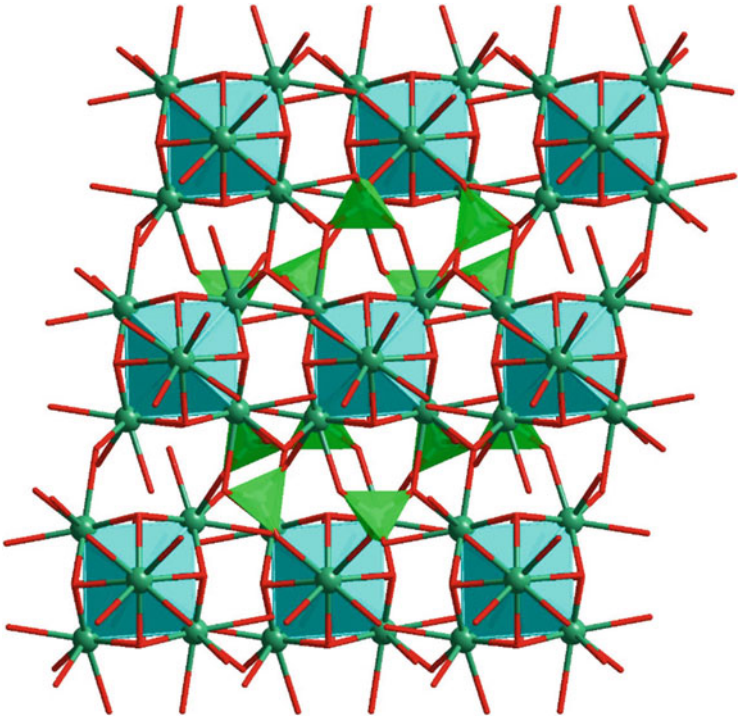

Fig. 13 Crystal structure of $[Gd_4(SO_4)_4(\mu_3\text{-}OH)_4(H_2O)_4]_n$ (**17**)

Based on the well-known octahedral $[Gd_6(\mu_6\text{-}O)(\mu_3\text{-}OH)_8]^{8+}$ nodes, a (3,12)-connected coordination polymer was solvothermally synthesized with the formula of $\{[Gd_6(\mu_6\text{-}O)(\mu_3\text{-}OH)_8(\mu_4\text{-}ClO_4)_4(H_2O)_6](OH)_4\}_n$ (**17**, Fig. 13) [27]. The large amount of inorganic component of this complex yields a very low $M\text{w}/N_{\text{Gd}}$ of 278.25 g mol^{-1}, which can lead to an upper limit for the $-\Delta S_{\text{M}}$ value of 62.13 J kg^{-1} K^{-1}. Unfortunately, the experimental value is much lower, namely 46.6 J kg^{-1} K^{-1}, at 2.5 K with $\Delta H = 70$ kOe and far from saturation with increasing fields. This is due mainly to the strong antiferromagnetic interactions between Gd(III) in this complex, characterized by a relatively large $\theta = -5.50$ K. However, the volumetric $-\Delta S_{\text{M}}$ value of up to 215.6 mJ cm^{-3} K^{-1} is still the largest among the 4f-clusters and 4f-cluster-based coordination polymers owing to the high mass density of 4.627 g cm^{-3}.

By hydrothermal reaction of Gd_2O_3, HNA and H_2DPA, the three-dimensional lanthanide framework, $[Gd_7(DPA)_5(NA)_3(\mu_3\text{-}OH)_8(H_2O)_3]\cdot 2.5H_2O$ (**18**), can be obtained [28]. Each heptanuclear $\{Gd_7(\mu_3\text{-}OH)_8\}$ core is formed by two vertex-sharing tetrahedral $\{Gd_4(\mu_3\text{-}OH)_4\}$ units, and the organic ligands further link them

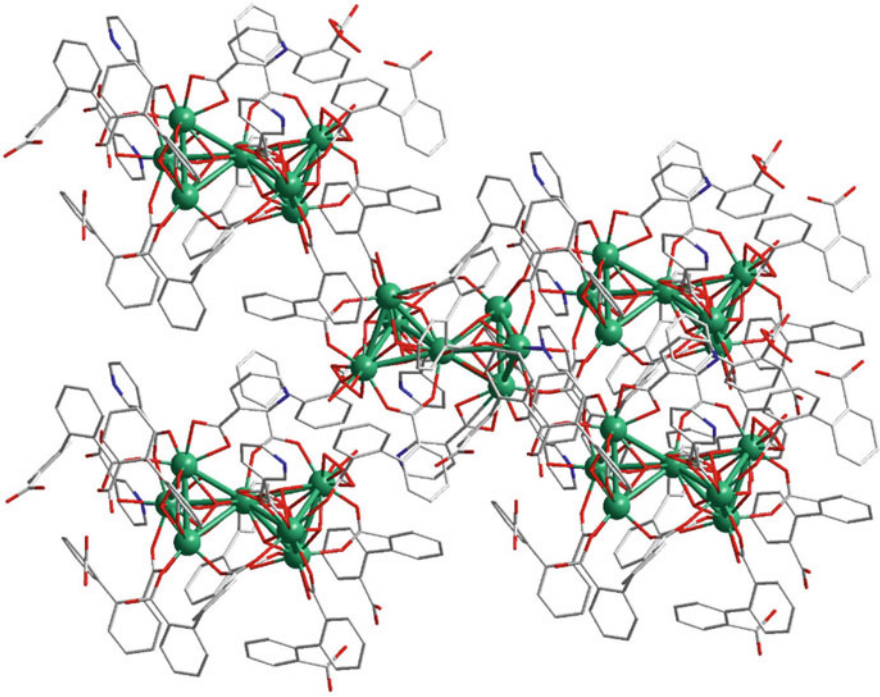

Fig. 14 Crystal structure of $[Gd_7(DPA)_5(NA)_3(\mu_3\text{-}OH)_8(H_2O)_3] \cdot 2.5H_2O$ (**18**)

into a four-connected **dia** net (Fig. 14). The magnetic interactions are antiferromagnetic with $\theta = -0.89$ K, and the maximum value of $-\Delta S_M$ is 34.2 J kg^{-1} K^{-1} at 2.5 K with $\Delta H = 70$ kOe.

The high-nuclearity clusters can also be connected by suitable ligands and extended into cluster-based coordination polymers. A novel two-dimensional coordination polymer, $[Gd_{36}(NA)_{36}(OH)_{49}(O)_6(NO_3)_6(N_3)_3(H_2O)_{20}]_nCl_{2n} \cdot 28nH_2O$ (**19**), is based on the $\{Gd_{36}\}$ clusters (Fig. 15) [29]. The maximum $-\Delta S_M$ value is 39.7 J kg^{-1} K^{-1} at 2.5 K with $\Delta H = 70$ kOe, lower than the limiting 49.64 J kg^{-1} K^{-1}, which is owing to the efficient antiferromagnetic interactions mediated by the OH^- and O^{2-} bridges with $\theta = -2.43$ K. Nevertheless, it provided a rare example of coordination polymers based on high-nuclearity clusters, and such types of compounds still have potential for the further improvement on their MCE (Table 1).

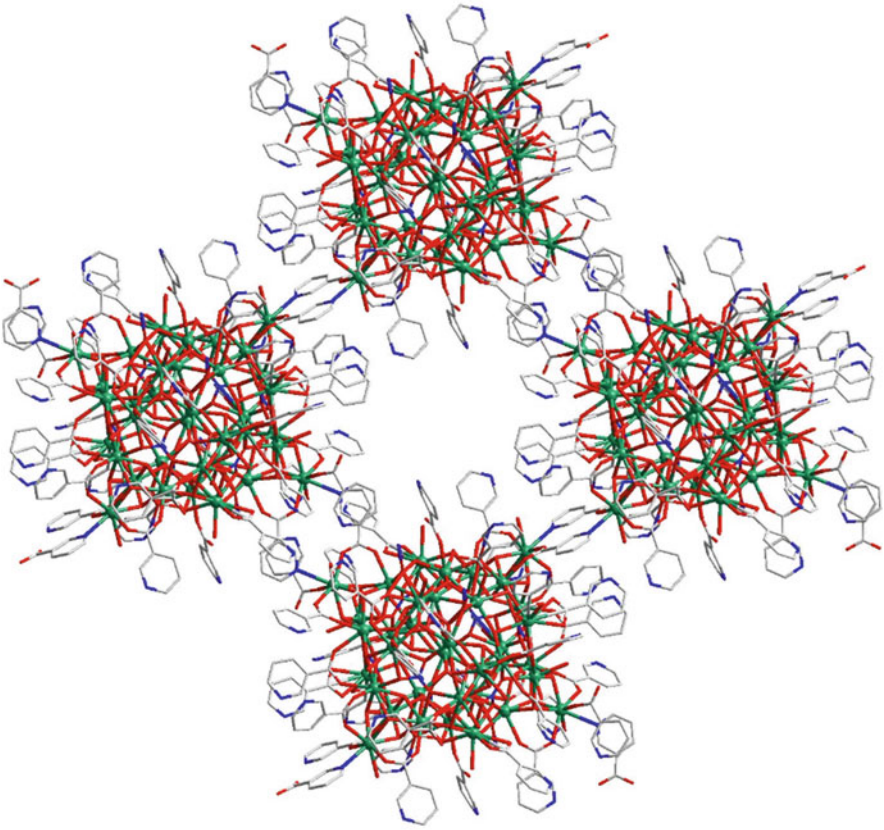

Fig. 15 Crystal structure of $[Gd_{36}(NA)_{36}(OH)_{49}(O)_6(NO_3)_6(N_3)_3(H_2O)_{20}]_nCl_{2n} \cdot 28nH_2O$ (**19**)

5 Conclusion and Outlook

As demonstrated above, a number of 4f-clusters for cryogenic magnetic cooling were reported just in the recent years, ranging from a simple dimer to a huge 104-nuclear cluster. However, most of them exhibit antiferromagnetic interactions between Gd(III) ions, with only a few exceptions [14–16]. Although the intra-cluster magnetic interactions are inevitable in these cluster compounds, they usually exhibit relatively weak inter-cluster magnetic interactions compared with most of the polymeric complexes with higher dimensionalities. As a result, the magnetic ordering temperature can be kept well below the working region for use as cryogenic magnetic coolants.

Many lessons on the magnetostructural correlations have been learned during the design and synthesis of these compounds, and the successful assembly strategies have been generalized and validated. Rational design and targeted synthesis shall

Table 1 $-\Delta S_M$ data at a given temperature with $\Delta H = 70$ kOe

Complex	$-\Delta S_M$		T/K	References
	J kg^{-1} K^{-1}	mJ cm^{-3} K^{-1}		
$[Gd_7(OH)_6(thmeH_2)_5(thmeH)(tpa)_6(MeCN)_2](NO_3)_2$ (**1**)	23	41.3	3	[13]
$[\{Gd(OAc)_3(H_2O)_2\}_2] \cdot 4H_2O$ (**2**)	40.6	82.8	1.8	[14]
$[Zn_2Gd_2(mvandeta)_2(CO_3)_2(NO_3)_2] \cdot 4CH_3OH$ (**3**)	18.5	31.0	1.9	[15]
$[Gd_2(OAc)_2(Ph_2acac)_4(MeOH)_2]$ (**4**)	23.7	60.1	2.4	[16]
$[Gd_4(OAc)_4(acac)_8(H_2O)_4]$ (**5**)	37.7	70.2	2.4	[16]
$[Gd_5O(O^iPr)_{13}]$ (**6**)	34	60.6	3	[17]
$[Gd_8(O_3P^tBu)_6(OH)_2(H_2O)_2(HO^iBu)(O_2C^tBu)_{12}](NH_3{}^iPr)_2$ (**7**)	32.3	45.0	3	[18]
$[Gd_{10}(3\text{-}TCA)_{22}(\mu_3\text{-}OH)_8(H_2O)_4]$ (**8**)	31.2	68.8	3	[19]
$[Gd_{10}(bmhcp)_5(\mu\text{-}OH)_6(H_2O)_{22}](Cl)_4 \cdot 7H_2O$ (**9**)	37.4	43.0	3	[20]
$[Gd_{12}Mo_4O_{16}(Hdhpimp)_6(OH)_4(OAc)_{12}] \cdot 12MeOH \cdot 8H_2O$ (**10**)	35.3	77.0	3	[21]
$[Gd_{24}(DMC)_{36}(CO_3)_{18}(H_2O)_2] \cdot 6H_2O$ (**11**)	46.1	89.9	2.5	[22]
$[Gd_{38}O(OH)_{42}(ClO_4)_6(CAA)_{37}(H_2O)_{36}(EtOH)_6](ClO_4)_{10}(OH)_{17} \cdot 14DMSO \cdot 13H_2O$ (**12**)	37.9	102	1.8	[23]
$[Gd_{48}O_6(OH)_{84}(CAA)_{36}(NO_3)_6(H_2O)_{24}(EtOH)_{12}(NO_3)Cl_2]Cl_3 \cdot 6DMF \cdot 5EtOH \cdot 20H_2O$ (**13**)	43.6	120.7	1.8	[23]
$[Gd_{104}(ClO_4)_6(CH_3COO)_{56}(\mu_3\text{-}OH)_{168}(\mu_4\text{-}O)_{30}(H_2O)_{112}](ClO_4)_{22} \cdot 2CH_3CH_2OH \cdot 140H_2O$ (**14**)	46.9	137.2	2	[24]
$[Gd_4(SO_4)_4(\mu_3\text{-}OH)_4(H_2O)]_n$ (**15**)	51.3	198.9	2	[25]
$[Gd_4(\mu_4\text{-}SO_4)_3(\mu_3\text{-}OH)_4(\mu\text{-}C_2O_4)(\mu\text{-}H_2O)(H_2O)_4]_n \cdot nH_2O$ (**16**)	51.5	190.5	2	[26]
$\{[Gd_6O(OH)_8(ClO_4)_4(H_2O)_6](OH)_4\}_n$ (**17**)	46.6	215.6	2.5	[27]
$[Gd_7(DPA)_5(NA)_3(\mu_3\text{-}OH)_8(H_2O)_3] \cdot 2.5H_2O$	34.2	74.7	2.5	[28]
$[Gd_{36}O_6(OH)_{49}(NA)_{36}(NO_3)_6(N_3)_3(H_2O)_{20}]_nCl_{2n} \cdot 28nH_2O$ (**19**)	39.7	91.3	2.5	[29]

be adopted in the future for high performance cryogenic magnetic coolants. For the 4f-cluster-based coordination polymers, although only a handful of cases have been reported, they have great potential to combine the advantages of discrete clusters and extended frameworks. Indeed, it has been evidenced that the 4f-based coordination polymers and even inorganics can have much superior magnetic cooling performance than any other kinds of materials ever reported [30–34], especially when there are ferromagnetic interactions such as in GdF_3 [35].

References

1. Debye P (1926) Ann Phys 386:1154
2. Giauque WF (1927) J Am Chem Soc 49:1864
3. Evangelisti M, Luis F, de Jongh LJ, Affronte M (2006) Magnetothermal properties of molecule-based materials. J Mater Chem 16(26):2534–2549
4. Evangelisti M, Brechin EK (2010) Recipes for enhanced molecular cooling. Dalton Trans 39:4672–4676
5. Gutfleisch O, Willard MA, Brück E, Chen CH, Sankar S, Liu JP (2011) Magnetic materials and devices for the 21st century: stronger, lighter, and more energy efficient. Adv Mater 23 (7):821–842
6. Sessoli R (2012) Chilling with magnetic molecules. Angew Chem Int Ed 51(1):43–45
7. Zheng Y-Z, Zhou G-J, Zheng Z, Winpenny RE (2014) Molecule-based magnetic coolers. Chem Soc Rev 43(5):1462–1475
8. Sharples JW, Collison D (2013) Coordination compounds and the magnetocaloric effect. Polyhedron 54:91–103
9. Shi PF, Xiong G, Zhang ZY, Zhao B (2013) Recent advance on molecule-based magnetic refrigeration materials at low temperatures. Scientia Sinica Chimica 43(10):1262–1271
10. Liu J-L, Chen Y-C, Guo F-S, Tong M-L (2014) Recent advances in the design of magnetic molecules for use as cryogenic magnetic coolants. Coord Chem Rev 281:26–49
11. Pecharsky VK, Gschneidner KA Jr (1999) Magnetocaloric effect and magnetic refrigeration. J Magn Magn Mater 200:44–56
12. Tishin AM, Spichkin YI (2003) The magnetocaloric effect and its applications. Institute of Physics, London
13. Sharples JW, Zheng Y-Z, Tuna F, McInnes EJ, Collison D (2011) Lanthanide discs chill well and relax slowly. Chem Commun 47(27):7650–7652
14. Evangelisti M, Roubeau O, Palacios E, Camon A, Hooper TN, Brechin EK, Alonso JJ (2011) Cryogenic magnetocaloric effect in a ferromagnetic molecular dimer. Angew Chem Int Ed 50 (29):6606–6609
15. Ruiz J, Lorusso G, Evangelisti M, Brechin EK, Pope SJ, Colacio E (2014) Closely-related $Zn^{II}_2Ln^{III}_2$ complexes (Ln^{III} = Gd, Yb) with either magnetic refrigerant or luminescent single-molecule magnet properties. Inorg Chem 53(7):3586–3594
16. Guo F-S, Leng J-D, Liu J-L, Meng Z-S, Tong M-L (2011) Polynuclear and polymeric gadolinium acetate derivatives with large magnetocaloric effect. Inorg Chem 51(1):405–413
17. Blagg RJ, Tuna F, McInnes EJL, Winpenny REP (2011) Pentametallic lanthanide-alkoxide square-based pyramids: high energy barrier for thermal relaxation in a holmium single molecule magnet. Chem Commun 47(38):10587–10589
18. Zangana KH, Pineda EM, Schnack J, Winpenny RE (2013) Octametallic 4f-phosphonate horseshoes. Dalton Trans 42(39):14045–14048
19. Liu S-J, Zhao J-P, Tao J, Jia J-M, Han S-D, Li Y, Chen Y-C, Bu X-H (2013) An unprecedented decanuclear GdIII cluster for magnetic refrigeration. Inorg Chem 52(16):9163–9165

20. Adhikary A, Jena HS, Khatua S, Konar S (2014) Synthesis and characterization of two discrete Ln10 nanoscopic ladder-type cages: magnetic studies reveal a significant cryogenic magnetocaloric effect and slow magnetic relaxation. Chem Asian J 9(4):1083–1090
21. Zheng Y, Zhang Q-C, Long L-S, Huang R-B, Müller A, Schnack J, Zheng L-S, Zheng Z (2013) Molybdate templated assembly of Ln 12 Mo 4-type clusters (Ln = Sm, Eu, Gd) containing a truncated tetrahedron core. Chem Commun 49(1):36–38
22. Chang L-X, Xiong G, Wang L, Cheng P, Zhao B (2013) A 24-Gd nanocapsule with a large magnetocaloric effect. Chem Commun 49(11):1055–1057
23. Guo F-S, Chen Y-C, Mao L-L, Lin W-Q, Leng J-D, Tarasenko R, Orendáč M, Prokleška J, Sechovský V, Tong M-L (2013) Anion-templated assembly and magnetocaloric properties of a nanoscale $\{Gd_{38}\}$ cage versus a $\{Gd_{48}\}$ barrel. Chem Eur J 19(44):14876–14885
24. Peng J-B, Kong X-J, Zhang Q-C, Orendáč M, Prokleška J, Ren Y-P, Long L-S, Zheng Z, Zheng L-S (2014) Beauty, symmetry, and magnetocaloric effect—four-shell keplerates with 104 lanthanide atoms. J Am Chem Soc 136(52):17938–17941
25. Han S-D, Miao X-H, Liu S-J, Bu X-H (2014) Magnetocaloric effect and slow magnetic relaxation in two dense (3,12)-connected lanthanide complexes. Inorg Chem Front 1 (7):549–552
26. Han S-D, Miao X-H, Liu S-J, Bu X-H (2014) Large magnetocaloric effect in a dense and stable inorganic–organic hybrid cobridged by in situ generated sulfate and oxalate. Chem Asian J 9 (11):3116–3120
27. Hou Y-L, Xiong G, Shi P-F, Cheng R-R, Cui J-Z, Zhao B (2013) Unique (3, 12)-connected coordination polymers displaying high stability, large magnetocaloric effect and slow magnetic relaxation. Chem Commun 49(54):6066–6068
28. Hu F-L, Jiang F-L, Zheng J, Wu M-Y, Pang J-D, Hong M-C (2015) Magnetic properties of 3D heptanuclear lanthanide frameworks supported by mixed ligands. Inorg Chem 54 (13):6081–6083
29. Wu M, Jiang F, Kong X, Yuan D, Long L, Al-Thabaiti SA, Hong M (2013) Two polymeric 36-metal pure lanthanide nanosize clusters. Chem Sci 4(8):3104–3109
30. Meng Y, Liu J-L, Zhang Z-M, Lin W-Q, Lin Z-J, Tong M-L (2013) Ionothermal synthesis of two oxalate-bridged lanthanide(iii) chains with slow magnetization relaxation by using a deep eutectic solvent. Dalton Trans 42(36):12853–12856
31. Chen Y-C, Guo F-S, Zheng Y-Z, Liu J-L, Leng J-D, Tarasenko R, Orendac M, Prokleska J, Sechovsky V, Tong M-L (2013) Gadolinium(III)-hydroxy ladders trapped in succinate frameworks with optimized magnetocaloric effect. Chem Eur J 19(40):13504–13510
32. Chen Y-C, Qin L, Meng Z-S, Yang D-F, Wu C, Fu Z, Zheng Y-Z, Liu J-L, Tarasenko R, Orendac M, Prokleska J, Sechovsky V, Tong M-L (2014) Study of a magnetic-cooling material $Gd(OH)CO_3$. J Mater Chem A 2(25):9851–9858
33. Meng Y, Chen Y-C, Zhang Z-M, Lin Z-J, Tong M-L (2014) Gadolinium oxalate derivatives with enhanced magnetocaloric effect via ionothermal synthesis. Inorg Chem 53 (17):9052–9057
34. Qiu JZ, Wang LF, Chen YC, Zhang ZM, Li QW, Tong ML (2016) Magneto-caloric properties of heterometallic 3d-Gd complexes based on the $[Gd(oda)_3]^{3-}$ metalloligand. Chem Eur J 22 (2):802–808. doi:10.1002/chem.201503796
35. Chen Y-C, Prokleška J, Xu W-J, Liu J-L, Liu J, Zhang W-X, Jia J-H, Sechovský V, Tong M-L (2015) A brilliant cryogenic magnetic coolant. Magnetic and magnetocaloric study of the ferromagnetically coupled GdF_3. J Mater Chem C 3(47):12206–12211